

# XAFS Spectroscopy of the Trichromium Acetate Aqueous Complex

M. Boyanov,<sup>1,2</sup> T. Shibata,<sup>1</sup> K. Kemner,<sup>2</sup> B. Bunker<sup>1</sup>

<sup>1</sup>Department of Physics, University of Notre Dame, Notre Dame, IN, U.S.A.

<sup>2</sup>Environmental Research Division, Argonne National Laboratory, Argonne, IL, U.S.A.

## Introduction

The structure of hydrated metal ions and their aqueous complexes has received increasing attention lately, as studies show that continuum models may not be adequate in explaining solution properties. Describing adsorption of solvated metal ions to mineral and biological surfaces also requires structural information, since the process is influenced by the metal's form and availability, which, in turn, depend on the complexes that the metal forms in solution. As part of our x-ray absorption fine structure (XAFS) spectroscopy studies on metals in solution [1], we have carried out experiments on aqueous Cr(III) in dilute perchlorate and acetate solutions. Chromium (Cr) takes part in a number of industrial processes as a dye, catalyst, or additive. From an environmental viewpoint, Cr, when it is at levels higher than trace concentrations, is hazardous, and its transport needs to be well understood. As a model for aqueous Cr interaction with organic matter, we have chosen the acetate group, since carboxyl binding centers are available in many cell surfaces and extracellular molecules that influence metal partitioning.

Several techniques have been used to characterize the hydrated Cr(III) ion: neutron scattering [2], x-ray scattering [3], and extended x-ray absorption fine structure (EXAFS) [4]. Results show that Cr(III) is octahedrally coordinated by six tightly bound water molecules at about 1.98 Å. Evidence of a second hydration sphere around Cr is found in the neutron scattering data. The ability of EXAFS to detect this shell has been discussed in some detail [4-6].

The aqueous acetate complexation of Cr(III) was studied by Fourier transform (FT) infrared spectroscopy [7]. On the basis of similarities in the aqueous and crystalline chromium acetate spectra, it was concluded that under the experimental conditions, the "molecule" present in the crystalline material was the same as that in solution. The structure is shown in Fig. 1. It is a trichromium complex that is bound together in a triangle by six bridging acetate groups and a central oxygen ion. Each Cr ion retains the octahedral oxygen coordination that it has as an individual ion in solution.

In this report, we present preliminary results from our XAFS study of the trichromium acetate aqueous complex. We observe significant changes in the x-ray absorption near-edge structure (XANES) region as the

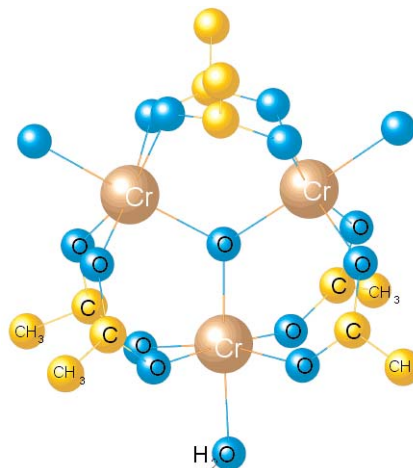


FIG. 1. Structure of the trichromium acetate complex in crystalline  $OCr_3(CH_3COO)_6 \cdot 3H_2O \cdot Cl \cdot 6H_2O$  [8].

local Cr environment gradually shifts from hydrated to acetate-bound. This is accompanied by a growing peak at around 3 Å in the Fourier transform, indicating Cr-Cr correlation. Initial modeling of the data is presented.

## Methods and Materials

As a model of hydrated Cr(III) ion, a 0.1 M chromium perchlorate aqueous solution was used. A series of 0.1 M aqueous Cr/acetate solutions with different acetate/Cr ratios and concentrations was prepared to observe the gradual shift in the equilibrium between hydrated and complexed cations toward the complexed species. The acetate samples were aged for 4 days so that the chromium triacetate complex could be formed [7]. Commercial perchlorate/acetate salts without further purification and 18 MΩ water were used for their preparation. Acetate group overloading of the solution was achieved by adding glacial acetic acid. The sample names reflect the acetate/Cr ratio (e.g., crac10 means an acetate/Cr ratio of 10).

The XAFS experiments were carried out at the MR-CAT beamline of the APS [9]. The beamline undulator was tapered, and the incident photon energy was scanned by using the (111) reflection of the Si double-crystal monochromator in quick-scanning mode (around 3 minutes per EXAFS scan and 1 minute per XANES scan). A Rh mirror was used for harmonic

rejection. Beam size was  $0.7 \times 0.7$  mm. The incident intensity did not vary more than 20% over the scanned energy range. The solutions were kept in Plexiglas® slides covered with Kapton® film windows during the measurements. Fluorescence detection with a Stern-Heald type assembly was employed. Energy calibration was continuously monitored during data collection.

Scans were aligned on the energy axis by the reference spectra and averaged. Background was subtracted by using the AUTOBK program [10]. Theoretical EXAFS calculations were obtained from the FEFF8 program [11], and the data were modeled by using FEFFIT [12].

## Results

Preliminary qualitative analysis of the XANES spectra and the FT of the EXAFS were included in the XAFS 12 conference proceedings [1]. We present them again here for completeness. Fig. 2 shows the change in the derivative of XANES spectra with increasing amounts of acetate ligands available in solution. The lines cross at isosbestic points, indicating that the spectra are composed of only two components by linear superposition: one corresponding to hydrated Cr, and one corresponding to Cr bound in the acetate complex. Fig. 3 shows the magnitude of the Fourier transform for the perchlorate (hydrated Cr) and acetate solutions. Distinct structure is observed at about 3 Å for the perchlorate solution. This is indicative of either a second hydration shell being detected or strong multiple scattering effects within the first hydration shell. The chromium acetate solutions show a peak above the hydrated Cr “baseline” features. The amplitude of the main FT peak is decreasing with acetate overloading of the solution, indicative of increased disorder in that

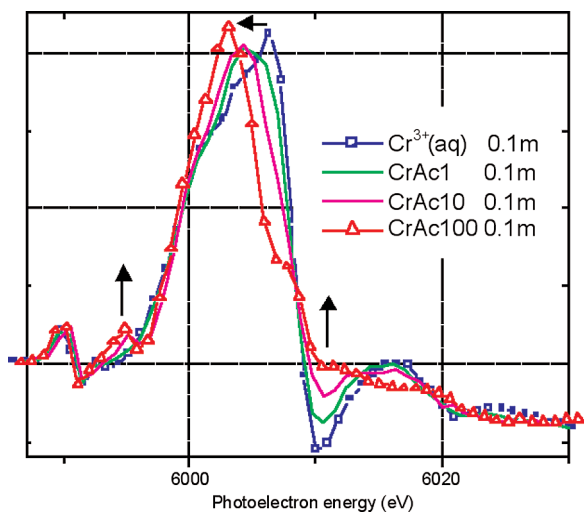


FIG. 2. Derivative of XANES spectra from the Cr perchlorate and acetate solutions.

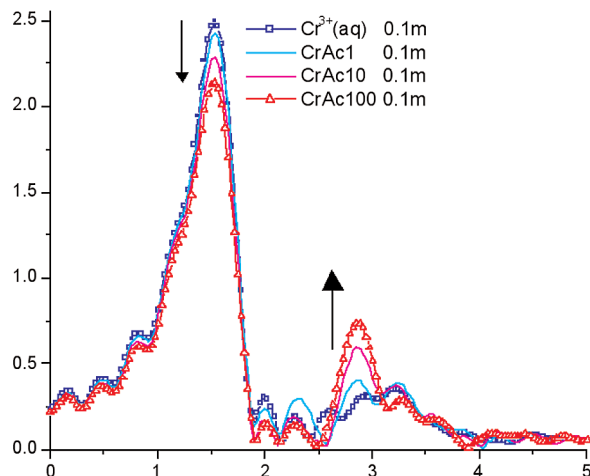


FIG. 3. Magnitude of the FT of  $k^2$ -weighted spectra from the Cr perchlorate and acetate solutions

shell or decreasing coordination number. The sharpness of the peak at 3 Å and its amplitude dependence on  $k$ -weighting of the FT (not shown) suggests an atom that is heavier than O or C, such as another Cr atom.

Numerical modeling of the EXAFS data has currently been completed only for the hydrated Cr spectrum. Results of the fits are presented in Table 1. The peak at 1.5 Å in the FT was successfully fit by an O shell containing six atoms at a distance of 1.97 Å. The peak at 3.0 Å could be fit by either 15 O atoms at 4.16 Å (outer hydration sphere) or by the multiple scattering contributions within the first shell. The quality of both fits, as judged by the goodness-of-fit values, is comparable. The fit using the multiple scattering paths within the first coordination shell was more constrained, since the number of these paths is related to the coordination number in the first shell. The large second shell disorder in the “outer hydration sphere” model prompted the use of a third cumulant to successfully reproduce the data.

## Discussion

Numerical modeling of the EXAFS data has currently been completed only for the hydrated Cr spectrum. Results of the fits are presented in Table 1. The peak at 1.5 Å in the FT was successfully fit by an O shell containing six atoms at a distance of 1.97 Å. The peak at 3.0 Å could be fit by either 15 O atoms at 4.16 Å (outer hydration sphere) or by the multiple scattering contributions within the first shell. The quality of both fits, as judged by the goodness-of-fit values, is comparable. The fit using the multiple scattering paths within the first coordination shell was more constrained, since the number of these paths is related to the coordination number in the first shell. The large second shell disorder in the “outer hydration

TABLE 1. Numerical results from fitting the hydrated Cr EXAFS data with two different models. Data are modeled in the range  $\Delta R = 1.0 - 4.0 \text{ \AA}$  and  $\Delta k = 2.5 - 12.5 \text{ \AA}^{-1}$ .  $N$  is the coordination number,  $R$  is the path length,  $\sigma^2$  is the Debye-Waller factor, and  $\Delta E_0$  is a shift in energy origin. The goodness-of-fit parameters ( $\chi_r^2$ ,  $R$ , and  $\gamma$ ) are explained in the FEFFIT documentation [12]. Path identification is O1 for the first hydration shell and O2 for the second; O11 for double scattering from the same atom; O12 and O13 for double and triple collinear scattering; and O14 for perpendicular triple scattering.

Shell	N	R(Å)	$\sigma^2(\text{Å}^2)$	$\Delta E_0(\text{eV})$
Second hydration shell model ( $\chi_r^2=138$ , $R=0.015$ , $\gamma=13$ )				
O1	5.9(3)	1.97(1)	0.0008(6)	2.2(6)
O2	15(5)	4.16(5)	0.02(1)	2.2(6)
		third cumulant->	0.011(3)	
First shell multiple scattering model ( $\chi_r^2=148$ , $R=0.018$ , $\gamma=15$ )				
O1	6.0(3)	1.96(1)	0.0010(6)	1.6(6)
O11	6.0(3)	4.01(2)	0.009(4)	1.6(6)
O12	6.0(3)	4.01(2)	0.009(4)	1.6(6)
O13	6.0(3)	4.01(2)	0.009(4)	1.6(6)
O14	6.0(3) x 4	4.01(2)	0.009(4)	1.6(6)

sphere” model prompted the use of a third cumulant to successfully reproduce the data.

The numerical results obtained from modeling the hydrated Cr(III) spectrum indicate a tightly bound octahedral hydration sphere at a distance of 1.97 Å. This distance is the same as that determined by previous neutron and x-ray scattering experiments and EXAFS studies. The small Debye-Waller factor is consistent with the observed long residence time of the water molecules in this shell. This strong interaction of Cr with its hydration sphere is also the likely reason that Cr acetate solutions need to be aged for several days in order for acetate complexation in solution to be observed [7]. The origin of the structure in the FT at 3.0 Å was the object of previous investigations [4-6]. The authors concluded that either single scattering from a second hydration shell alone, or the latter combined with multiple scattering within the first shell, can fit the data in this region, but multiple scattering alone cannot. We tested single scattering from the second O shell and multiple scattering within the first O shell, and both fit the data equally well in that region. Since the two have quite similar signatures in the FT, testing them together will not be conclusive because of the overlapping contributions. We favor the multiple-scattering interpretation, since the tightly bound first coordination sphere (confirmed by first-shell EXAFS results) is likely to result in significant multiple-scattering

contributions. The second hydration sphere, on the other hand, is likely to have a broad distribution of Cr-O distances, resulting in loss of coherence in the backscattered electron waves.

## Acknowledgments

Boyanov thanks the Bayer Corp. for its support through a Bayer predoctoral fellowship. Help from the MR-CAT beamline staff is acknowledged, as is J. Fein for use of his laboratory. Work at Notre Dame was supported in part by the National Science Foundation through Grant No. NSF-EAR99-05704. Work performed at MR-CAT is supported in part by funding from DOE Grant No. DE-FG02-00ER45811. Use of the APS was supported by the DOE Office of Science, Office of Basic Energy Sciences, under Contract No. W-31-109-ENG-38. Support for Kemner was provided by the DOE Office of Science, Office of Biological and Environmental Research, Natural and Accelerated Bioremediation Research (NABIR) Program.

## References

- [1] M.I. Boyanov, T. Shibata, S.D. Kelly, K.M. Kemner, and B.A. Bunker, in *Physica Scripta, Proceedings of the XAFS 12 Conference in Malmo, Sweden* (submitted 2003).
- [2] R.D. Broadbent, G.W. Neilson, and M. Sandstrom, *J. Phys. Condens Matter* **4**, 639 (1992).
- [3] R. Caminiti, G. Licheri, G. Piccaluga, and G. Pinna, *Chem. Phys.* **19**, 371 (1977).
- [4] A. Munoz-Paez, R.R. Pappalardo, and E.S. Marcos, *J. Am. Chem. Soc.* **117**, 11710 (1995).
- [5] S. Diaz-Moreno, A. Munoz Paez, J.M. Martinez, R.R. Pappalardo, and E.S. Marcos, *J. Am. Chem. Soc.* **118**, 12654 (1996).
- [6] H. Sakane et al., *J. Am. Chem. Soc.* **120**, 10397 (1998).
- [7] J.E. Tackett, *Appl. Spectrosc.* **43**, 490 (1989).
- [8] S.C. Chang and G.A. Jeffrey, *Acta Crystallogr.* **B26**, 673 (1970).
- [9] C.U. Segre et al., “The MRCAT insertion device beamline at the Advanced Photon Source,” in *Synchrotron Radiation Instrumentation: Eleventh U.S. National Conference*, edited by P. Pianetta (American Institute of Physics, New York, NY, 2000), p. 419.
- [10] M. Newville, P. Livins, Y. Yacoby, J.J. Rehr, and E.A. Stern, *Phys. Rev. B* **47**, 14126 (1993).
- [11] A.L. Ankudinov, B. Ravel, J.J. Rehr, and S.D. Conradson, *Phys. Rev. B* **58**, 7565 (1998).
- [12] M. Newville, *FEFFIT: Using FEFF to Model XAFS Data*, part of program documentation provided with FEFFIT (1998).